NIH Public Access
Author Manuscript
ChemMedChem. Author manuscript; available in PMC 2014 June 09.

Published in final edited form as:
ChemMedChem. 2012 March 5; 7(3): 452–463. doi:10.1002/cmdc.201100568.

CHROMENOPYRAZOLES: NON-PSYCHOACTIVE AND SELECTIVE CB_1 CANNABINOID AGONISTS WITH PERIPHERAL ANTINOCICEPTIVE PROPERTIES

Jose Cumella Dr.[a], **Laura Hernández-Folgado Dr.**[a], **Rocio Girón Dr.**[b], **Eva Sánchez Dr.**[b], **Paula Morales**[a], **Dow P. Hurst Dr.**[c], **Maria Gómez-Cañas Dr.**[d], **Maria Gómez-Ruiz**[d], **Diana C. G. A. Pinto Dr.**[e], **Pilar Goya Dr.**[a] **[Prof.]**, **Patricia H. Reggio Dr.**[c] **[Prof.]**, **María Isabel Martin Dr.**[b] **[Prof.]**, **Javier Fernández-Ruiz Dr.**[d] **[Prof.]**, **Artur M. S. Silva Dr.**[e] **[Prof.]**, and **Nadine Jagerovic Dr.**[*,a]

[a]Instituto de Química Médica, CSIC, Juan de la Cierva 3, 28006, Madrid (Spain)

[b]Departamento de Farmacología y Nutrición, Facultad de Ciencias de la Salud, Universidad Rey Juan Carlos, Avda. Atenas S/N, 28922 Alcorcón, Madrid (Spain)

[c]Department of Chemistry and Biochemistry, University of North Carolina Greensboro, Greensboro NC27402 (USA)

[d]Departamento de Bioquímica y Biología Molecular, Facultad de Medicina, Centro de Investigación Biomédica en Red sobre Enfermedades Neurodegenerativas (CIBERNED), Instituto Ramón y Cajal de Investigación Sanitaria (IRYCIS), Universidad Complutense de Madrid, 28040 Madrid (Spain)

[e]Department of Chemistry & QOPNA, University of Aveiro, 38210-193 Aveiro (Portugal)

Abstract

The unwanted psychoactive effects of cannabinoid receptor agonists have limited their development as medicines. These CB_1 mediated side effects are due to the fact that CB_1 receptors are largely expressed in the Central Nervous System (CNS). Since it is known that CB_1 receptors are also located peripherally, there is a growing interest in targeting cannabinoid receptors located outside the brain. A library of chromenopyrazoles designed in analogy to the classical cannabinoid cannabinol were synthesized, characterized and tested for cannabinoid activity. Radiolabeled binding assays were used to determine their affinities at CB_1 and CB_2 receptors. Structural features required for CB_1/CB_2 affinity and selectivity were explored using molecular modeling. Within the chromenopyrazoles series, some of them showed to be selective CB_1 ligands. These modeling studies suggest that CB_1 full selectivity over CB_2 can be accounted for the presence of a pyrazole ring in the structure. The functional activities of selected chromenopyrazoles were evaluated in isolated tissues. Behavioral tests, in vivo, were then carried on the most effective CB_1 cannabinoid agonist (**13a**). Chromenopyrazole **13a** did not induce modifications in any of the tested parameters on the mouse cannabinoid tetrad, discarding CNS-mediated effects. This lack of agonistic activity in the CNS suggests that it does not readily cross the blood-brain barrier.

[*]nadine@iqm.csic.es.

NIH-PA Author Manuscript
NIH-PA Author Manuscript
NIH-PA Author Manuscript

NIH-PA Author Manuscript

NIH-PA Author Manuscript

NIH-PA Author Manuscript

Moreover, compound **13a** can induce antinociception in a peripheral model of orofacial pain in rat. Taking into account the negative results obtained in the hot plate test, it could be suggested that the antinociception induced by **13a** in the orofacial test may be mediated through peripheral mechanisms.

Keywords

agonist; cannabinoid; peripheral; protein model; receptor

Introduction

The three major components of marijuana are Δ^9-tetrahydrocannabinol (Δ^9-THC), cannabidiol (CBD) and cannabinol (CBN).[1] Unlike Δ^9-THC,[2] CBD and CBN are nonpsychotropic phytocannabinoids.[3] Δ^9-THC interacts with two well-characterized G protein-coupled receptors, CB_1 and $CB1_2$.[4-5] The CB_1 receptors are localized with high density in the brain and are also found in peripheral tissues. On the other hand, the CB_2 receptors are expressed mainly in immune cells, although they were also found in CNS particularly under pathological circumstances. The activity of the cannabinoid receptors is elicited not only by phytocannabinoids, but also by synthetic ligands and endocannabinoids.[6-9] The only cannabinoid receptor ligands prescribed so far are CB_1/CB_2 receptor agonists. Cesamet® (nabilone) and Marinol® (Δ^9-THC) are used for the treatment of nausea and vomiting associated with cancer chemotherapy or as anti-emetic agents. Sativex® (Δ^9-THC and CBD) is prescribed to relieve spasticity and pain of multiple sclerosis patients. However, preclinical data indicate that CB_1 and/or CB_2 receptor agonists are useful with diverse therapeutic applications that include pain relief, treatment of intestinal disorders, glaucoma, cancer proliferation and neurodegenerative diseases.[10-12]

Δ^9-THC and CBN are classical cannabinoids characterized by tricyclic terpenoids bearing a benzopyran moiety (Figure 1).[13] Structure-activity relationships (SARs) of Δ^9-THC and Δ^8-THC analogues for CB_1/CB_2 receptors have been widely reported.[14-19] It is well-established that C-1, C-3, and C-9 positions play a key role in binding affinity and pharmacological potency of THCs. Even though some of these classical cannabinoids have been reported to show significant selectivity for one of the two receptor types, structural variations within Δ^9-THC generally resulted in derivatives with high affinity for both CB_1 and CB_2 receptors. Considerable effort has been directed toward the SARs of THCs; however less structural modifications have been made on the structure of cannabinol. Rhee *et al.* [20] reported binding evaluation and inhibition of adenylylcyclase data of a series of CBN derivatives. Unlike CBN that was found to be less potent than Δ^9-THC, the 3-dimethylheptyl CBN analogue and the 9-hydroxymethyl CBN analogues showed more affinity and agonist potency than Δ^9-THC at both CB_1 and CB_2 receptors. The presence of alkyl or aryl esters in position 9 of CBN resulted in weak CB_1 and CB_2 binding.[21] More recently, cannabilactones have been reported by Khanolkar *et al.* [22] One of them exhibited high CB_2 receptor affinity with 500-fold selectivity over CB_1 receptor. Taking together all these considerations, it is clear that structural requirement for cannabinoid receptors binding of CBN series differs from THCs.

NIH-PA Author Manuscript

NIH-PA Author Manuscript

NIH-PA Author Manuscript

The pharmacological properties of CBN have also received less attention than the THCs. Analgesic properties of CBN have been reported in different models of pain.23-26] [Thus, CBN generally needed higher doses than Δ^9-THC to produce antinociception but it showed minimal psychomimetic effects.[27-28] One of the main challenges at designing new cannabinoid ligands is to develop cannabinoids devoid of CNS side effects. In 1985 Press *et al.* [29] published benzopyrano[4,3-*c*]pyrazoles that did not show neuroleptic activity in the locomotor and catalepsy tests. We propose to explore this scaffold for cannabinoid ligands. In this context, we report here the contribution of a pyrazole ring in replacement of the cannabinol phenyl group to cannabinoid activity.

Chemistry

7-Alkyl-1,4-dihydro-4,4-dimethylchromenopyrazol-9-oles **7-15** were prepared from the corresponding resorcinol following Scheme 1. Resorcinol 5-(1′,1′-dimethylheptyl)-1,3-dihydroxybenzene (**2**) was previously synthesized by demethylation[30] of 5-(1′,1′-dimethylheptyl)-1,3-dimethoxybenzene. The appropriate starting resorcinol reacted with 3,3-dimethylacrylic acid in methanesulfonic acid in presence of phosphorus pentoxide to form the 7-alkyl-5-hydroxy-2,2-dimethylchroman-4-ones **3** and **4** in microwave heating conditions and using the reagents described by Lim *et al.*[31] For the α–formylation of **3-4**, an alternative procedure to the overnight heating proposed by Press[32] yielded the corresponding (*Z*)-7-alkyl-5-hydroxy-3-(hydroxymethylen)-2,2-dimetylchroman-4-ones **5** and **6** in 20 min using microwave irradiation. Then condensation of the *β*–ketoaldehydes **5** and **6** with the appropriate hydrazine gave the corresponding 7-alkyl-1(2),4-dihydro-4,4-dimethylchromeno[4,3-*c*]pyrazol-9-oles **7-15**. From methyl- and ethylhydrazines, the two N^1- and N^2-substituted pyrazole isomers (**8a**,**b**; **9a**,**b**; **13a,b**) were isolated with an approximate relative from 8:2 to 6:4 ratio (N^1:N^2). However, when the *β*–ketoaldehyde **5** or **6** reacted with arylhydrazine only one isomer could be isolated corresponding to the N^1-aryl chromenopyrazole (**10a**, **14a** and **15a**). The fact that alkylhydrazines give a mixture of N^1- and N^2-substituted 7-alkyl-1(2),4-dihydro-4,4-dimethylchromeno[4,3-*c*]pyrazol-9-oles can be explained by the reaction of *N*′-hydrazine but also of *N*-hydrazine with the aldehyde group of **5** and **6** giving upon cyclization compounds **8a**,**b**; **9a**,**b** and **13a**,**b**. The nucleophilicity of *N*′-hydrazine is much lesser than that of *N*-hydrazine in the case of *N*′-aryl hydrazines and this leads to a single isomer as in the case of **10a**, **14a** and **15a**.

Biological results

Competitive binding studies

The compounds reported here were evaluated in vitro for their ability to displace [^{3}H]-CP55,940 from human cannabinoid CB_1 and CB_2 receptors transfected into HEK293 EBNA cells. They were first subjected to a preliminary screening at a concentration of 40 μM. A complete dose-response curve was carried out for compounds that displaced the radioligand by more than 50% in the preliminary screenning. Table 1 lists the experimental binding affinities (K_i) from the respective displacement curves for *h*CB_1 and *h*CB_2 receptors.

The first series to be examined were the 2,4-dihydrochromen[4,3-*c*]pyrazol-9-oles and 1,4-dihydrochromen[4,3-*c*]pyrazol-9-oles bearing a *n*-pentyl side chain (**7-10a**). Excluding **10a**

NIH-PA Author Manuscript

NIH-PA Author Manuscript

NIH-PA Author Manuscript

that binds weakly to the CB_1 cannabinoid receptor, the binding data for **7**, **8a**, **8b**, **9a** and **9b** (Table 1) clearly show that they failed to bind to either CB_1 or CB_2 receptors. As reported in the literature,[33] the introduction of C1′-alkyl substituent to Δ^9-THC, Δ^8-THC and cannabinol derivatives leads to enhancement in affinity for both receptors, CB_1 and CB_2. Interestingly, the 1,1-dimethylheptyl chromenopyrazole derivatives **11**, **12b**, **13a, 13b,** and **15a** showed significant to high affinity for CB_1 (CB_1: K_i = 4.5-28.5 nM) while they did not bind to the CB_2 receptor at all (CB_2: K_i > 40000 nM). So far such CB_1 receptor selectivity has never been observed among the cannabinoid ligands with a classical cannabinoid structure. Thus, chromenopyrazoles **11**, **12b**, **13a, 13b,** and **15a** showed an optimal CB_1 selectivity compared to CB_1/CB_2 binding data reported for Δ^9-THC, Δ^8-THC and cannabinol derivatives.

With respect to the substitution modification on the pyrazole ring, the K_i value remained substantially comparable in the 1,1-dimethylheptyl analogues, except for the N^1-3,4-dichlorophenyl moiety which compound (**14a**) exhibited reduced affinity for both receptors, CB_1 and CB_2 , with a loss of CB_1 selectivity.

Isolated tissues assays

The functional activity of **11, 13a** and **13b** was tested on mouse vas deferens, a tissue commonly used to study and characterize cannabinoid effects, where CB_1 cannabinoid receptors are expressed, as previously described.[34]

Compounds **11**, **13a** and **13b** inhibited electrically evoked contractile response of this tissue. In agreement with its high affinity for the CB_1 type, **13a** exhibited the highest effectiveness (Figure 2). These three ligands were less effective than WIN55212-2 (WIN); however, their effect was comparable to that of arachidonyl-2-chloroethylamide (ACEA), a CB_1 selective agonist commonly used to characterize cannabinoid effects. Considering that compound **13a** showed the most interesting profile as potential CB_1 agonist, the inhibition of its effect was tested adding to the organ bath the cannabinoid antagonist AM251, 10 min before the addition of the tested compound. As it is illustrated in Figure 3, the effect of **13a** was clearly decreased by the selective CB_1 antagonist AM251. Moreover, the CB_2 antagonist AM630 was also tested but it did not block **13a** effect (data not shown).

In vivo bioassays: Cannabinoid tetrad

Psychoactive cannabinoids dose-dependently modify spontaneous activity, antinociceptive response, rectal temperature, and catalepsy in mice.[35] Effects of WIN and **13a** on the cannabinoid tetrad were evaluated. Intraperitoneal (i.p.) administration of WIN (2.5 and 5 mg/kg) induced antinociceptive effect in the hot-plate test, hypothermia, catalepsy and reduction of the locomotor activity, whereas compound **13a** (5 and 10 mg/kg) did not modify any of the signs of cannabinoid tetrad (Figure 4). This result suggests that **13a** lacks of significant central effects.

In vivo bioassays: Orofacial pain model

Hyper tonic saline (HS) injection in the masseter of rats produced a paw shaking behavior. This nociceptive behavior was reduced by the intraperitoneal (i.p.) administration of

NIH-PA Author Manuscript

NIH-PA Author Manuscript

NIH-PA Author Manuscript

compound **13a** (1 and 3 mg/kg), suggesting that **13a** is active in this pain model (Figure 5), acting at CB_1 receptors located outside the CNS.

Molecular Modeling

The CB_1 cannabinoid receptor selectivity observed for the 1,1-dimethylheptyl chromenopyrazoles offers us the opportunity to explore structural features required for CB_1/CB_2 selectivity using molecular modeling.

Conformational analysis of the *N*-H-chromenopyrazole **11** and the two *N*-CH_3-chromenopyrazole regioisomers **13a** and **13b** were first performed to determine the global minimum energy conformation of each and other minimum energy conformations. With respect to the *N*-H-chromenopyrazole **11**, two tautomers (**11a** and **11b** in Figure 6) were considered. Even though the conformational analysis of **11a** showed that it was more stable than **11b** by 1.9 kcal/mol, both tautomers were taken into consideration for docking studies.

Figure 7 illustrates the global minimum energy conformers of tautomers **11a** and **11b**, and regioisomers **13a** and **13b**.

The global energy minima of **11a**, **11b**, **13a** and **13b** were then docked using a model of the activated state (R*) of the cannabinoid receptors CB_1 and CB_2.[36-37] These models include the extracellular and intracellular loops, the N-terminus (truncated in CB1) and the C-terminus, including the intracellular helix portion of each receptor, termed Helix 8. CB_1 and CB_2 receptor docking studies were performed in the same binding site described for HU-210[38] and for AM-841[39-40] respectively.

Chromenopyrazole tautomer 11b/ CB_1R* Cannabinoid Receptor Docking Studies

The energy minimized **11b**/CB_1R* complex is illustrated in Figure 8. Lys3.28(192) was used as the primary interaction site in CB_1 docking studies reported here.[41] The phenolic oxygen of **11b** is engaged in hydrogen bond with Lys3.28(192) as reported for HU-210/CB_1R* binding model [Hydrogen bond (N-O) distance = 2.78 Å and (N-H--O) angle = 150°]. The N^2-pyrazole nitrogen is involved in hydrogen bond with Ser7.39(383) [Hydrogen bond (N-O) distance = 3.15 Å and (O-H--N) angle = 142°]. The ligand **11b** exhibits the greatest pair-wise interaction energy with Lys3.28(192) (−11.88 kcal/mol), followed by Leu7.43(387) (−5.64 kcal/mol), Cys7.42(386) (−5.61 kcal/mol) and Asn7.45(389) (−5.43 kcal/mol). Coulombic energy dominates the overall pair-wise energy of interaction in the case of Lys3.28(192), while van der Waals energy is predominant for Leu7.43(387), Cys7.42(386) and Asn7.45(389). The interaction with Ser7.39(383) was found to be only −4.48 kcal/mol indicating a weak hydrogen bond with the N^2-pyrazole nitrogen. The tautomer **11b** also has significant interactions with Asp2.50(163) (−4.99 kcal/mol) with van der Waals and coulombic contributions, and with Val3.32(196) (−4.97 kcal/mol), whose interaction is dominated by van der Waals interactions. The energy difference between the initially docked **11b** conformation and the final conformation in the energy-minimized complex was found to be 6.69 kcal/mol at the Hartree-Fock (HF) 6-31G* level. The overall interaction energy for **11b** at CB_1 was found to be −56.52 kcal/mol (see Table S1 in Supporting Information).

NIH-PA Author Manuscript

NIH-PA Author Manuscript

NIH-PA Author Manuscript

Chromenopyrazole tautomer 11a/ CB_1R* Cannabinoid Receptor Docking Studies

The docking of the tautomer **11a** in CB_1R* receptor model revealed a similar occupation of the binding site with similar hydrogen bonds involving Lys 3.28(192) and Ser7.39(383) as shown in Figure 8. As for **11b**/CB_1R* complex, **11a** has the greatest pair-wise interaction energy with Lys3.28(192) (−11.02 kcal/mol), and significant interactions with Cys7.42(386) (−6.22 kcal/mol), Asp2.50(163) (−6.03 kcal/mol), Leu7.43(387) (−5.20 kcal/mol), Asn7.45(389) (−5.13 kcal/mol) and Val3.32(196) (−4.40 kcal/mol). However, the interaction energy with Ser7.39(383) (−10.88 kcal/mol) in the **11a**/CB_1R* complex was found much stronger than for **11b**. The energy difference between the initially docked **11a** conformation and the final conformation in the energy-minimized complex was found to be 6.51 kcal/mol at the HF 6-31G* level. The overall interaction energy for **11a** at CB_1 was found to be −63.92 kcal/mol (see Table S1 in Supporting Information).

Taken together, the energies of interaction of **11a** and **11b** at CB_1 suggest that **11a** is the preferred tautomeric form for **11** binding at CB_1.

Chromenopyrazole 13b/ CB_1R* Cannabinoid Receptor Docking Studies

In the energy minimized **13b**/CB_1R* complex as illustrated in Figure 9, **13b** forms two hydrogen bonds with Lys 3.28(192). The first involved Lys 3.28(192) as hydrogen donor to the phenolic oxygen of **13b** [Hydrogen bond (N-O) distance = 2.75 Å and (N-H--O) angle = 152°]). The second interaction involved Lys 3.28(192) hydrogen bonding with the pyrazole N^2 nitrogen [Hydrogen bond (N-N) distance = 3.10 Å and (N-H--N) angle = 132°]. This pyrazole N^2 nitrogen also forms a hydrogen bond with Ser7.39(383) [Hydrogen bond (N-O) distance = 3.15 Å and (O-H--N) angle =134°]. However, this interaction is weaker than in the CB_1R* complex with **11** and **13a**. The ligand **13b** has its greatest pair-wise interaction energy with Lys3.28(192) (−14.34 kcal/mol, mainly coulombic energy), followed by Asn7.45(389) (−5.19 kcal/mol), Leu7.43(387) (−5.13 kcal/mol) and Cys7.42(386) (−4.76 kcal/mol) which are predominantly van der Waals energy. The **13b**/CB_1R* complex also has significant interactions with Val3.32(196) (−4.72 kcal/mol) and Asp2.50(163) (−4.70 kcal/mol). The energy difference between the initially docked **13b** conformation and the final conformation in the energy-minimized complex was found to be 5.13 kcal/mol at the HF 6-31G* level. The overall interaction energy for **13b** at CB_1 was found to be −59.92 kcal/mol (see Table S2 in Supporting Information).

Chromenopyrazole 13a/ CB_1R* Cannabinoid Receptor Docking Studies

The main interactions of the energy minimized **13a**/CB_1R* complex are shown on Figure 9. As observed for **11a**, **11b** and **13b**, Lys 3.28(192) forms hydrogen bond with the phenolic oxygen of **13a** [Hydrogen bond (N-O) distance = 2.70 Å and (N-H--O) angle = 166°]. The N^2 of the pyrazole of **13a** hydrogen bonds with Ser7.39(383), as a hydrogen bond acceptor [Hydrogen bond (N-O) distance = 2.80 Å and (O-H--N) angle = 160°]. It is interesting to note that an additional hydrogen bond between the pyran ring oxygen and Cys7.42(386) was revealed in the **13a**/CB_1R* complex [Hydrogen bond (S-O) distance = 2.91 Å and (S-H-O) angle = 172°]. The significant increase in pair-wise interaction energy with Cys7.42(386) (−7.01 kcal/mol) compared to the other complexes presented here (**11a**,**11b** and **13b**) is a

NIH-PA Author Manuscript

NIH-PA Author Manuscript

NIH-PA Author Manuscript

consequence of this additional hydrogen bond. The ligand **13a** exhibits greatest interaction energy with Lys3.28(192) (−13.83 kcal/mol), followed by the hydrogen bond interaction with Ser7.39(383) (−7.47 kcal/mol) and Phe2.57(170) (−5.30 kcal/mol). The Phe2.57(170) interaction has significant van der Waals and coulombic contributions and seems to have arisen from the interaction of the phenolic ring hydrogens with the aromatic ring of the phenylalanine. The **13a**/CB_1R* complex also has significant interactions with Leu7.43(387) (−7.43 kcal/mol), Asp2.50(163) (−6.22 kcal/mol), Asn7.45(389) (−4.97 kcal/mol) and Val3.32(196) (−4.94 kcal/mol). The energy difference between the initially docked **13a** conformation and the final conformation in the energy-minimized complex was found to be 7.39 kcal/mol at the HF 6-31G* level. The overall interaction energy for **13a**, at CB_1 was found to be −69.16 kcal/mol (see Table S2 in Supporting Information).

Taken together with results for **13b** above, docking studies indicate that the interaction of **13a** at CB_1 is more energetically favorable than those of its positional isomer.

Chromenopyrazoles 11a/, 11b/, 13a/ and 13b/ CB_2R* Cannabinoid Receptor Docking Studies

Compounds**11a, 11b**, **13b** and **13a** were also docked in the previously reported advanced CB_2R* model[37,40,42] at the AM-841 binding site[40]. The CB_2 receptor model contains a salt bridge between D275 (Asp275) in the EC-3 loop and K3.28 Lys3.28(109). Docking studies of the chromenopyrazoles **11a**, **11b**, **13a** and **13b** revealed a steric clash between the pyrazole moiety of the structures and the ionic lock as illustrated in Figure 10.

This result suggests that the presence of the pyrazole plays a key role in the selectivity of compounds **11** and **13** for CB_1cannabinoid receptor.

Discussion and Conclusion

Even though the first generation of classical cannabinoids showed potent activity in vivo, they lacked CB_1 or CB_2 selectivity and most of them are psychoactive. These CB_1 mediated side effects are due to the fact that CB_1 receptors are largely expressed in the CNS. Thus, the unwanted psychoactive effects of cannabinoid receptor agonists have limited their development as medicines. Since it is known that CB_1 receptors are also located peripherally,[43] there is a growing interest in targeting cannabinoid receptors located outside the brain. For this reason, it is important to develop new nonpsychoactive cannabinoids that do not cross the blood-brain barrier but act on peripherally located cannabinoid receptors. The chromenopyrazoles presented here were designed in analogy to CBN, which is a CB_1/CB_2 cannabinoid ligand. The binding data show that the 1,1-dimethylheptyl side chain on this scaffold is necessary for high affinity. The ligand binding studies resulted in K_i values of 4.5 - 28.5 nM for the 1,1-dimethylheptyl analogues (**11**, **12b**, **13a, 13b,** and **15a**) at *h*CB_1 receptors. Worth of note is that these 1,1-dimethylheptyl analogues did not have any affinity for *h*CB_2 receptors (K_i > 40000 nM). Unlike the major members of the classical cannabinoid family that lack CB_1 or CB_2 full selectivity, chromenopyrazoles structure have a determinant influence on CB_1 selectivity. These results suggest that such selectivity can be accounted by the presence of a pyrazole ring in the structure. However, the substituent on the pyrazole may play a major role in the binding to

NIH-PA Author Manuscript

NIH-PA Author Manuscript

NIH-PA Author Manuscript

both receptors. Thus, we observed that 1-(3,4-dichlorophenyl) substituent (**14a**) disturbed significantly the CB_1 receptor selectivity with a loss of affinity for CB_1 and a moderate affinity for CB_2 receptor.

As assessed by modeling studies, the 1,1-dimethylheptylchromenopyrazoles **11a**, **11b**, **13a** and **13b** revealed a similar occupation of the HU-210/CP55,940 binding site in the CB_1 receptor model. The phenolic hydroxyl group of **11a**, **11b**, **13a** and **13b** is crucial for the interaction with CB_1R^*, due to a hydrogen bond with Lys3.28(192). This residue has been shown to be critical for the binding of both classical and endocannabinoids.[41] Furthermore, interaction with Ser7.39(383) was found as the main one for the pyrazole moiety, in particular for the **13a**/CB_1R^* complex. This residue (Ser7.39(383)) has been reported to be crucial for the binding of the CB_1 agonist, CP55,940.[38]

While K3.28 in CB_1 has been reported to be critical for the binding of non-classical, classical and endocannabinoids,[41] mutation of the equivalent residue in CB_2, K3.28(109) has no effect on the binding of any cannabinoid ligand.[44] An important sequence divergence in the EC-3 loop of the CB_2 model (TTLS**D**QVKK) vs CB_1 model (GKMN**K**LIKT) has been reported.[40] The CB_2R^* model suggests a salt bridge formed between Asp275 and Lys3.28(109) that makes K3.28 unavailable for ligand interaction. In our CB_2R^* dock, this salt bridge causes a steric clash with the pyrazole moiety of **11a**, **11b**, **13a** or **13b** due to the rigidity and planarity of the heterocycle. Therefore, these results suggest that the pyrazole moiety in these compounds is responsible for the CB_1 selectivity over CB_2.

Compounds **13a** and **13b** are positional isomers of one another differing in the placement of an ethyl substituent (N^1-, **13a**; N^2-, **13b**). It is interesting to note that the interaction energies of **13a** and **13b** with CB_1 calculated here follow the same trend as their CB_1 affinities (**13a**, E_{int} = −69.16 kcal/mol, K_i = 4.5nM vs **13b**, E_{int} = −59.92 kcal/mol, K_i = 18.6nM).

The chromenopyrazoles **11**, **13a** and **13b** were tested in functional in vitro assays, where from all of them, **13a** acted as the most effective cannabinoid agonist. Its effect was significantly and almost completely inhibited by the CB_1 antagonist AM251 but not by the CB_2 antagonist AM630.

Then, **13a** was selected to carry on behavioral tests, in vivo, in which it did not induce modifications in any of the tested parameters on the mouse cannabinoid tetrad, discarding CNS-mediated effects. This lack of agonistic activity in the CNS suggests that they do not readily cross the blood-brain barrier.

To study other possibility of antinociception, compound **13a** was tested in another pain model. We chose a model of orofacial pain in rat (nocive stimulation of the masseter by injection of hypertonic saline); it is known that, in this model, other drugs, such as opioids, can induce antinociception by peripheral mechanisms.[45-46] In this test, **13a** was able to reduce the nociceptive response. It is interesting to remark the different result obtained using this test with respect to the results recorded when the hot plate test was performed. From

NIH-PA Author Manuscript

NIH-PA Author Manuscript

NIH-PA Author Manuscript

these data it could be suggested that the antinociception induced by compound **13a** in the orofacial test may be mediated through peripheral mechanisms.

Experimental Section

Chemistry

Commercially available starting materials and reagents were used as supplied. Reactions conducted under anhydrous condition were performed under nitrogen atmosphere in solvents dried over $CaCl_2$ (THF) or Na/benzophenone (THF). Microwave-mediated syntheses were performed using 800W Ethos Synth microwave (Milestone Inc.) and CEM Biotage microwave. Column chromatography was performed using silica gel 60 (230-400 mesh). Analytical HPLC/MS analysis was performed on a Waters 2695 HPLC system equipped with a Photodiode Array 2996 coupled to Micromass ZQ 2000 mass spectrometer (ESI-MS), using a Waters X-bridge C18 column (3.5 μm, 2.1 × 100 mm) and 30 min gradient A: MeCN/0.08% formic acid, B: H_2O/0.05% formic acid visualizing at λ = 254 nm. ^1H and ^{13}C NMR spectra were recorded on a Bruker 300 (300 and 75 MHz) at 25°C. Samples were prepared as solutions in deuterated solvent and referenced to internal nondeuterated solvent peak. Chemical shifts were expressed in ppm (δ) downfield of tetramethylsilane. Elemental analyses were determined by LECO CHNS-932. Melting points were determined on MP70 Reichert Jung Thermovar apparatus and are uncorrected. The purity of final compounds was determined by HPLC/MS analyses using above-mentioned instrument and by elemental analyses performed with LECO CHNS-932 analyzer.

5-(1,1-Dimethylheptyl)-1,3-dihydroxybenzene[30] (2)

To a solution of 5-(1,1-dimethylheptyl)-1,3-dimethoxybenzene (0.45 g, 1.9 mmol) in dry CH_2Cl_2 was added boron tribromide (1M in CH_2Cl_2) (19 mL, 19 mmol) at −16 °C under nitrogen in the dark. The reaction mixture was allowed to warm to room temperature and was stirred for 20 h. Then MeOH was added carefully at 0 °C until pH = 7. The solvent was removed in vacuo and the crude was purified by chromatography on silica gel (EtOAc) to give the title compound as a white solid (0.33 g, 73%); mp: 88-91 °C (98 °C)[30]; ^1H NMR ($CDCl_3$): δ = 6.35-6.45 (m, 2H, 4-H), 6.16 (m, 1H, 2-H), 4.65 (bs, 2H, OH), 1.45-1.50 (m, 2H, 2′-H), 1.22 (s, 6H, CH_3), 1.21-1.10 (m, 6H, 3′-H, 4′-H, 5′-H,), 1.03 (bs, 2H, 6′-H), 0.84 (t, *J* = 6.5 Hz, 3H, CH_3); ^{13}C NMR ($CDCl_3$): δ = 163.2 (3-C), 154.0 (5-C), 111.2 (4-C), 101.3 (2-C)), 45.0 (2′-C), 35.3, 31.1, and 23.9 (3′-C, 4′-C, 5′-C) , 29.8 (8′-C), 25.1 (6′-C), 14.8 (7′-C); HPLC/MS: [A, 20% - 80%], Rt = 14.0 min, (90%); MS (ES^+, m/z) 237 (100%) $[M+H]^+$; Anal. calcd. for $C_{15}H_{24}O_2$: C 76.23, H 10.24, found: C 76.10, H 10.18.

5-Hydroxy-2,2-dimethyl-7-pentylchroman-4-one[29] (3)

To a mixture of phosphorus pentoxide (0.23 g, 1.6 mmol) and methanesulfonic acid (4.6 mL, 72 mmol) was added olivetol (0.48 g, 2.7 mmol) and 3,3-dimethylacrylic acid (0.27 g, 2.7 mmol) under nitrogen at room temperature. Then the mixture was irradiated by microwave at 70 °C in a sealed reactor for 10 min. The mixture was poured onto water/ice then it was extracted with CH_2Cl_2. The organic layer was dried over $MgSO_4$. After removal of the solvent, the crude was purified by chromatography on silica gel (EtOAc) to give the

NIH-PA Author Manuscript

NIH-PA Author Manuscript

NIH-PA Author Manuscript

title compound as a orange oil (0.34 g, 48%); ^{1}H NMR ($CDCl_3$): δ = 6.32 (d, *J* = 2.4 Hz, 1H, 8-H), 6.26 (d, *J* = 2.4 Hz, 1H, 6-H), 2.98 (t, *J* = 7.1 Hz, 2H, 1′-H), 2.66 (s, 2H, 3-H), 1.48-1.53 (m, 2H, 2′-H), 1.44-1.38 (m, 2H, 3′-H), 1.41 (s, 6H, $OC(CH_3)_2$), 1.30-1.40 (m, 2H, 4′-H), 0.87 (t, *J* = 6.9 Hz, 3H, 5′-H); ^{13}C NMR ($CDCl_3$): δ = 191.2 (4-C), 161.9 (5-C), 159.7 (8a-C), 147.6 7-C), 110. 2 (8-C), 109.9 (6-C), 100.1 (4-C), 76.4 (2-C), 48.3 (3-C), 33.3 (1′-C), 30.1 (3′-C), 28.1 (2′-C), 24.8 ($OC(CH_3)_2$), 20.7 (4′-C), 12.2 (5′-C); HPLC/MS: [A, 20% - 80%], Rt = 17.6 min, (90%); MS (ES^+, m/z) 263 (100%) $[M+H]^+$; Anal. calcd. for $C_{16}H_{22}O_3$: C 73.25, H 8.45, found: C 72.98, H 8.71.

7-(1,1-Dimethylheptyl)-5-hydroxy-2,2-dimethylchroman-4-one (4)

Prepared from **2** (0.37 g, 1.6 mmol), phosphorus pentoxide (0.18 g, 1.3 mmol), methanesulphonic acid (2.67 mL, 54 mmol) and 3,3-dimethylacrylic acid (1.99 g, 19.9 mmol) following the procedure described for **3**. Yellowish oil (0.34 g, 40%); ^{1}H NMR ($CDCl_3$): δ = 6.45 (d, *J* = 1.6 Hz, 1H, 8-H), 6.37 (d, *J* = 1.6 Hz, 1H, 6-H), 2.71 (s, 2H, 3-H), 1.52-1.59 (m, 2H, 2′-H), 1.46 (s, 6H, $OC(CH_3)_2$), 1.22 (s, 6H, $C(CH_3)_2$), 1.19 (bs, 6H, 3′-H, 4′-H, 5′-H), 1.05 (bs, 2H, 6′-H), 0.87 (m, 3H, 7′-H); ^{13}C NMR ($CDCl_3$): δ = 197.9 (4-C), 163.0 (5-C), 161.7 (8a-C), 156.0 (7-C), 107.0 (8-C), 106.2 (6-C), 105.7 (4-C), 79.1 (2-C), 48.5 (3-C), 41.0 (2′-C), 39.2 (1′-C), 32.1, 27.1 and 23.0 (3′-C, 4′-C and 5′-.C), 30.3 ($C(CH_3)_2$), 28.8 ($OC(CH_3)_2$), 25.0 (6′-C), 14.5 (7′-C); HPLC/MS: [A, 80% - 100%], Rt = 4.9 min, (97%); MS (ES^+, m/z) 318 (97%) $[M+H]^+$; Anal. calcd. for $C_{20}H_{30}O_3$: C 75.43, H 9.50, found: C 75.52, H 9.64.

5-Hydroxy-3-(hydroxymethylen)-2,2-dimethyl-7-pentyl-chroman-4-one[29] (5)

To a solution of the dihydrochroman-4-one **3** (0.17 g, 0.7 mmol) in dry THF was added dry 95% sodium hydride (0.14 g, 6 mmol) under nitrogen. The reaction mixture was irradiated by microwave at 46 °C in a sealed reactor for 20 min. Then ethyl formate (0.96 mL, 12 mmol) was added and the mixture was irradiated for an additional 20 min at 46 °C. The solvent was then evaporated under reduced pressure. Water was added to the residue. The aqueous solution was extracted with Et_2O then it was neutralized with 1M HCl and extracted with CH_2Cl_2. The combined organic layers were dried anhydride $MgSO_4$ and evaporated under reduced pressure. Column chromatography on silica gel (Hex/EtOAc, 1/1) afforded the titled compound as a yellowish oil (0.12 g, 60%); ^{1}H NMR ($CDCl_3$): δ = 13.48 (d, *J* = 11.1 Hz, 1H, CHO*H*), 11.36 (s, 1H, 5-OH), 7.34 (d, *J* = 11.1 Hz, 1H, 10-H), 6.32 (d, *J* = 1.3 Hz, 1H, 8-H), 6.21 (d, *J* = 1.3 Hz, 1H, 6-H), 2.49 (t, *J* = 7.6 Hz, 2H, 1′-H), 1.58-1.65 (m, 2H, 2′-H), 1.56 (bs, 6H, 9-H), 1.30-1.19 (m, 4H, 3′-H and 4′-H), 0.88 (t, *J* = 7.2 Hz, 3H, 5′-H); ^{13}C NMR ($CDCl_3$): δ = 189.9 (4-C), 162.3 (5-C), 161.9 (CHOH), 159.3 (8a-C), 155.9 (7-C), 114.7 (3-C), 109.8 (8-C), 108.7 (6-C), 105.5 (4-C), 78.7 (2-C), 37.1 (1′-C)), 31.8 (3′-C), 30.4 (2′-C), 28.6 (9-C), 22.9 (4′-C), 14.4 (5′-C). MS (ES^+, m/z) 291 (100%) $[M+H]^+$; HPLC/MS: [A, 80% - 100%], Rt = 1.5 min, (99%); MS (ES^+, m/z) 318 (97%) $[M+H]^+$; Anal. calcd. for $C_{17}H_{22}O_4$: C 70.32, H 7.64, found: C 70.47, H 7.31.

7-(1,1-Dimethylheptyl)-5-hydroxy-3-(hydroxymethylen)-2,2-dimethylchroman-4-one (6)

Prepared from **4** (0.17 g, 0.5 mmol), sodium hydride (0.16 g, 6.7 mmol) and ethyl formate (1.44 mL, 2.7 mmol) following the procedure described for **5**. Column chromatography on

NIH-PA Author Manuscript

NIH-PA Author Manuscript

NIH-PA Author Manuscript

silica gel (Hex/EtOAc, 2/1). Yellowish oil (0.16 g, 76%); ^{1}H NMR ($CDCl_3$): δ = 13.48 (d, *J* = 11.6 Hz, 1H, CHO*H*), 11.28 (s, 1H, 5-OH), 7.34 (d, *J* = 11.6 Hz, 1H, C*H*OH), 6.46 (d, *J* = 1.6 Hz, 1H, 8-H), 6.35 (d, *J* = 1.6 Hz, 1H, 6-H), 1.58 (bs, 6H, $OC(CH_3)_2$), 1.22 (bs, 6H, $C(CH_3)_2$), 1.12-1.28 (m, 6H, 3′-H, 4′-H and 5′-H), 1.03 (m, 2H, 6′-H), 0.83 (t, *J* = 6.7 Hz, 3H, 7′-H); ^{13}C NMR ($CDCl_3$): δ = 189.8 (4-C), 163.1 (5-C), 162.0 (CHOH), 161.9 (8a-C), 159.1 (7-C), 114.8 (3-C), 107.8 (6-C), 106.6 (8-C), 105.2 (4-C), 78.7 (2-C), 44.4 (2′-C), 39.2 (1′-C), 32.1, 30.3 and 25.0 (3′-C, 4′-H and 5′-H), 28.8 ($C(CH_3)_2$), 28.6 ($OC(CH_3)_2$), 23.0 (6′-C), 14.5 (7′-C); HPLC/MS: [A, 20% - 80%], Rt = 22.7 min, (100%); MS (ES^+, m/z) 347 (100%) $[M+H]^+$; Anal. calcd. for $C_{21}H_{30}O_4$: C 72.80, H 8.73, found: C 73.07, H 8.64.

1,4-Dihydro-4,4-dimethyl-7-pentylchromen[4,3-*c*]pyrazol-9-ol (7)

A solution of **5** (40 mg, 0.13 mmol) and anhydrous hydrazine (10 mg, 0.26 mmol) in EtOH (3 mL) was irradiated under microwave for 10 min. The solvent was evaporated and the crude residue was chromatographied on silica gel (Hex/EtOAc, 2/1) to obtain **7** as a white solid (20 mg, 59%); mp: 133-137 °C; ^{1}H NMR ($CDCl_3$): δ = 8.52 (bs, 1H, OH), 7.31 (s, 1H, 3-H), 6.44 (d, *J* = 1.5 Hz, 1H, 6-H), 6.37 (d, *J* = 1.5 Hz, 1H, 8-H), 2.53 (t, *J* = 7.1 Hz, 2H, 1′-H), 1.90-1.76 (m, 8H, $OC(CH_3)_2$ and 2′-H), 1.41-1.31 (m, 4H, 3′-H and 4′-H), 0.86 (t, *J* = 6.9 Hz, 3H, 5′-H); ^{13}C NMR ($CDCl_3$): δ = 156.1 (9-C), 153.9 (5a-C), 146.3 (7-C), 142.7 (9b-C), 123.4 (3-C), 120.2 (3a-C), 109.4 (6-C), 108.6 (8-C), 101.7 (9a-C), 77.0 (4-C), 36.6 (1′-C), 31.9 (3′-C), 30.9 (2′-C), 29.9 ($OC(CH_3)_2$), 22.9 (4′-C), 14.4 (5′-C); HPLC/MS: [A, 10% - 100%], Rt = 5.9 min, (98%). MS (ES^+, m/z) 287 (97%) $[M+H]^+$; Anal. calcd. for $C_{17}H_{22}N_2O_2$: C 71.30, H 7.74, found: C 71.01, H 7.47.

1,4-Dihydro-1,4,4-trimethyl-7-pentylchromeno[4,3-*c*]pyrazol-9-ol[29] (8a) and 2,4-dihydro-2,4,4-trimethyl-7-pentylchromeno[4,3-*c*]pyrazol-9-ol[29] (8b)

To a solution of **5** (10 mg, 0.03 mmol) in EtOH was added methylhydrazine (7.00 μL, 0.13 mmol). The reaction mixture was stirred at room temperature for 16 h. The solvent was evaporated under reduced pressure. The crude oil was purified by column chromatography on silica gel (Hex/EtOAc, 2/1) to isolate the two isomers **8a** and **8b**. **8a** was obtained as an orange oil (4 mg, 39%); ^{1}H NMR ($CDCl_3$): δ = 7.32 (s, 1H, 3-H), 6.50 (d, *J* = 1.3 Hz, 1H, 6-H), 6.27 (d, *J* = 1.3 Hz, 1H, 8-H), 4.11 (s, 3H, N-CH_3), 2.50 (t, *J* = 7.7 Hz, 2H, 1′-H), 1.55-1.44 (m, 8H, 2′-H and $OC(CH_3)_2$), 1.31-1.25 (m, 4H, 3′-H and 4′-H), 0.89 (m, 3H, 5′-H); ^{13}C NMR ($CDCl_3$): δ = 154.5 (9-C), 149.9 (5a-C), 145.4 (7-C), 132.0 (9b-H), 130.9 (3-C)), 123.1 (3a-C), 111.4(8-C), 109.5 (6-C), 76.4 (4-C), 41.1 (N-CH_3), 38.7 (1′-C), 35.7 (3′-C), 31.4 (2′-C), 27.3 ($OC(CH_3)_2$), 22.5 (4′-C), 14.0 (5′-C); HPLC/MS: [A, 20% - 80%], Rt = 15.1 min, (95%); MS (ES^+, m/z) 301 (100%) $[M+H]^+$; Anal. calcd. for $C_{19}H_{26}N_2O_2$: C 72.58, H 8.33, found: C 72.81, H 8.26. **8b** was obtained as a yellowish oil (6 mg, 58%); ^{1}H NMR ($CDCl_3$): δ = 8.31 (s, 1H, OH), 7.09 (s, 1H, 3-H), 6.42 (d, *J* = 1.1 Hz, 1H, 6-H), 6.34 (d, *J* = 1.1 Hz, 1H, 8-H), 3.90 (s, 3H, N-CH_3), 2.50 (t, *J* = 7.6 Hz, 2H, 1′-H), 1.59 (bs, 6H, $OC(CH_3)_2$), 1.50-1.60 (m, 2H, 2′-H), 1.30-1.18 (m, 4H, 3′-H and 4′-H), 0.95-0.84 (m, 3H, 5′-H); ^{13}C NMR ($CDCl_3$): δ = 153.6 (9-C), 153.1 (5a-C), 145.3 (7-C), 142.6 (9b-C), 124.0 (3a-C), 120.3 (8-C), 108.7 (6-C), 108.5 (9a-C), 101.5(9a-C), 76.4(4-C), 38.8 (N-CH_3), 36.2 (1′-C), 31.5 and 22.5 (3′-C and 4′-C), 30.7 (2′-C), 29.6 ($OC(CH_3)_2$), 14.0 (5′-C); HPLC/MS: [A, 20% - 80%], Rt = 19.9 min, (96%); MS (ES^+, m/z) 301 (100%) $[M+H]^+$; Anal. calcd. for $C_{19}H_{26}N_2O_2$: C 72.58, H 8.33, found: C 72.36, H 8.49.

NIH-PA Author Manuscript

NIH-PA Author Manuscript

NIH-PA Author Manuscript

1-Ethyl-1,4-dihydro-4,4-dimethyl-7-pentylchromeno[4,3-*c*]pyrazol-9-ol (9a) and 2-Ethyl-2,4-dihydro-4,4-dimethyl-7-pentylchromeno[4,3-*c*]pyrazol-9-ol (9b)

A solution of **5** (40 mg, 0.15 mmol) and ethylhydrazine oxalate (20 mg, 0.15 mmol) in EtOH (3 mL) was irradiated under microwave for 10 min. The solvent was evaporated and the crude residue was chromatographied on silica gel (Hex/EtOAc, 1/1) to isolate the two isomers **9a** and **9b**. **9a** was obtained as a yellowish oil (6.0 mg, 12%)**;** ^{1}H NMR ($CDCl_3$): δ = 9.35 (bs, 1H, OH), 7.38 (s, 1H, 3-H), 6.46 (s, 1H, 6-H), 6.45 (s, 1H, 8-H), 4.48 (q, *J* = 7.1 Hz, 2H, NCH_2CH_3), 2.50 (t, *J* = 7.6 Hz, 2H, 1′-H), 1.66-1.52 (m, 8H, 2′-H and $OC(CH_3)_2$), 1.43 (t, *J* = 7.1 Hz, 3H, NCH_2CH_3), 1.28-1.19 (m, 4H, 3′-H and 4′-H), 0.88 (t, *J* = 6.7 Hz, 3H, 5′-H); ^{13}C NMR ($CDCl_3$): δ = 155.5 (9-C), 151.8 (5a-C), 145.6 (7-C), 132.9 (9b-C), 131.7 (3-C), 122.9 (3a-C), 110.4 (6-C), 109.7 (8-C), 103.1 (9a-C), 76.04(4-C), 48.0 (NCH_2CH_3), 35.7 (1′-C), 31.4 and 22.5 (3′-C and 4′-C), 30.4 (2′-C), 27.2 ($OC(CH_3)_2$), 15.9 (NCH_2CH_3), 14.0 (5′-C); HPLC/MS: [A, 60% - 100%], Rt = 1.6 min, (100%); MS (ES^+, m/z) 315 (100%) $[M+H]^+$; Anal. calcd. for $C_{23}H_{34}N_2O_2$: C 74.55, H 9.25, found: C 74.63, H 9.19. **9b** was obtained as a yellow solid (0.04 g, 61%); m.p. = 145-149 °C; ^{1}H NMR ($CDCl_3$): δ = 8.38 (s, 1H, OH), 7.12 (s, 1H, 3-H), 6.42 (d, *J* = 1.3 Hz, 1H, 6-H), 6.30 (d, *J* = 1.3 Hz, 1H, 8-H), 4.17 (q, *J* = 7.1 Hz, 2H, NCH_2CH_3), 2.50 (t, *J* = 7.1 Hz, 2H, 1′-H), 1.58-1.53 (m, 8H, 2′-H and $OC(CH_3)_2$), 1.48 (t, *J* = 7.1 Hz, 3H, NCH_2CH_3), 1.30-1.19 (m, 4H, 3′-H and 4′-H), 0.95-0.81 (m, 3, 5′-H); ^{13}C NMR ($CDCl_3$): δ = 153.5 (9-C), 153.0 (5a-C), 145.2 (7-C)), 142.4 (9b-C), 122.3 (3-C), 119.8 (3a-C), 108.7 (8-C), 108.4 (6-C), 101.6 (9a-C), 76.7 (4-C), 47.0 (NCH_2CH_3), 36.2 (1′-C), 31.4 and 22.5 (3′-C and 4′-C), 30.7 (2′-C), 29.6 ($OC(CH_3)_2$), 15.4 (NCH_2CH_3), 14.0 (5′-C); HPLC/MS: [A, 60% - 100%], Rt = 2.3 min, (100%); MS (ES^+, m/z) 315 (100%) $[M+H]^+$; Anal. calcd. for $C_{23}H_{34}N_2O_2$: C 74.55, H 9.25, found: C 74.23, H 9.41.

1-(3,4-Dichlorophenyl)-1,4-dihydro-4,4-dimethyl-7-pentylchromeno[4,3-*c*]pyrazol-9-ol (10b)

Prepared from **5** (14 mg, 0.05 mmol) and 3,4-dichlorophenylhydrazine hydrochloride (10 mg, 0.05 mmol) following the procedure described for **7**. Column chromatography on silica gel (Hex/EtOAc, 2/1) afforded **10b** as an orange solid (7 mg, 31%); mp: 120-124°C; ^{1}H NMR ($CDCl_3$): δ = 7.57 (d, *J* = 2.4 Hz, 1H, 2-Hphenyl), 7.49 (s, 1H, 3-H), 7.44 (d, *J* = 8.7 Hz, 1H, 5-H_{phenyl}), 7.24 (dd, *J* = 2.4 Hz, *J* = 8.7 Hz, 1H, 6-H_{phenyl}), 6.52 (d, *J* = 1.2 Hz,1H, 6-H), 6.10 (d, *J* = 1.2 Hz, 1H, 8-H), 2.53-2.45 (m, 2H, 1′-H), 1.60-1.51 (m, 8H, 2′-H and $OC(CH_3)_2$), 1.30-1.22 (m, 4H, 3′-H and 4′-H), 0.93-0.88 (m, 3H, 5′-H); ^{13}C NMR ($CDCl_3$): δ = 154.5 (9-C), 150.0 (5a-C), 146.3 (7-C), 142.0 (1-C_{phenyl}), 137.9 (3-C), 132.9 (3-C_{phenyl}), 132.2 (9b-C), 131.0 (4-C_{phenyl}), 129.9 (5-C_{phenyl}), 126.0 (2-C_{phenyl}), 124.9 (3a-C), 123.5 (6-C_{phenyl}), 111.2 (8-C), 109.7 (6-C), 102.3 (9a-C), 77.2 (4-C), 36.7 (1′-C), 31.5 and 22.5 (3′-C and 4′-C), 30.3 (2′-C), 27.2 ($OC(CH_3)_2$), 14.0 (5′-C); HPLC/MS: [A, 60% - 100%], Rt = 2.3 min, (100%); MS (ES^+, m/z) 431 (100%) $[M+H]^+$.

1,4-Dihydro-4,4-dimethyl-7-(1,1-dimethylheptyl)chromeno[4,3-*c*]pyrazol-9-ol (11)

Prepared from **6** (16 mg, 0.05 mmol) and anhydrous hydrazine (0.01 mL, 0.32 mmol) following the procedure described for **7**. Column chromatography on silica gel (Hex/EtOAc, 2/1) afforded **11** as an orange oil (7 mg, 41%); ^{1}H NMR ($CDCl_3$): δ = 7.32 (bs, 1H, NH), 6.58 (d, *J* = 1.5 Hz, 1H, 6-H), 6.51 (d, *J* = 1.5 Hz, 8-H), 6.48 (s, 1H, 3-H), 1.63 (bs, 6H,

NIH-PA Author Manuscript

NIH-PA Author Manuscript

NIH-PA Author Manuscript

$OC(CH_3)_2$), 1.58-1.52 (m, 2H, 2′-H), 1.25 (s, 6H, $C(CH_3)_2$), 1.18 (bs, 6H, 3′-H, 4′-H and 5′-H), 1.12-1.05 (m, 2H, 6′-H), 0.83 (t, *J* = 6.7 Hz, 3H, 7′-H); ^{13}C NMR: δ = ($CDCl_3$) 153.7 (9-C), 153.5 (5a-C), 153.4 (7-C), 144.1 (9b-C), 129.1 (3-C), 123.4 (3a-C), 106.8 (8-C), 106.5 (6-C), 101.7 (9a-C), 77.0 ($OC(CH_3)_2$), 44.9 (2′-C), 38.4 ($C(CH_3)_2$), 32.2, 30.4, and 30.0 (3′-C, 4′-C and 5′-C), 29.3 ($C(CH_3)_2$), 25.0 ($OC(CH_3)_2$), 23.1 (6′-C), 14.5 (7′-C); HPLC/MS: [A, 80% - 100%], Rt = 3.1 min, (100%); MS (ES^+, m/z) 343 (100%) $[M+H]^+$; Anal. calcd. for $C_{21}H_{30}N_2O_2$: C 73.65, H 8.83, found: C 74.01, H, 8.59.

7-(1,1-Dimethylheptyl)-2,4-dihydro-2,4,4-trimethylchromeno[4,3-*c*]pyrazol-9-ol (12b)

Prepared from **6** (30 mg, 0.09 mmol) and methylhydrazine (0.02 mL, 0.34 mmol) following the procedure described for **7**. Column chromatography on silica gel (Hex/EtOAc, 2/1) afforded **12b** as a yellow solid (13 mg, 42%); mp > 300°C; ^{1}H NMR ($CDCl_3$): δ = 8.23 (s, 1H, OH), 7.09 (s, 1H, 3-H), 6.57 (d, *J* = 1.6 Hz, 1H, 6H), 6.48 (d, *J* = 1.6 Hz, 1H, 8-H), 3.90 (s, 3H, NCH_3), 1.63 (s, 6H, $OC(CH_3)_2$), 1.65-1.54 (m, 2H, 3′-H), 1.24 (s, 6H, $C(CH_3)_2$), 1.18-1.09 (m, 6H, 3′-H, 4′-H and 5′-H), 1.10-1.04 (m, 2H, 6′-H), 0.83 (t, *J* = 6.7 Hz, 3H, 7′-H); ^{13}C NMR ($CDCl_3$): δ = 152.2 (9-C), 151.8 (5a-C), 151.6 (7-C), 141.5 (9b-C), 122.9 (3-C), 119.3 (3a-C), 105.5 (6-C), 105.3 (8-C), 100.2 (9a-C), 76.4 ($OC(CH_3)_2$), 43.5 (NCH_3), 38.9 (2′-C), 38.0 (1′-C), 31.8, 30.0 and 29.7 (3′-C, 4′-C and 5′-C), 28.9 (8′-C), 24.6 ($OC(CH_3)_2$), 22.6 (6′-C), 14.1 (7′-C); HPLC/MS: [A, 80% - 100%], Rt = 5.9 min, (100%); MS (ES^+, m/z) 357 (100%) $[M+H]^+$.

7-(1,1-Dimethylheptyl)-1-ethyl-1,4-dihydro-4,4-dimethylchromeno[4,3-*c*]pyrazol-9-ol (13a) and 7-(1,1-dimethylheptyl)-2-ethyl-2,4-dihydro-4,4-dimethylchromeno[4,3-*c*]pyrazol-9-ol (13b)

Prepared from **6** (35 mg, 0.1 mmol) and ethylhydrazine oxalate (15.00 mg, 0.1 mmol) following the procedure described for **9a/9b**. Column chromatography on silica gel (Hex/EtOAc, 2/1) allowed isolating the two isomers **13a** and **13b**. **13a** was obtained as a yellowish oil (5.00 mg, 18%); ^{1}H NMR ($CDCl_3$): δ = 8.77 (bs, 1H, OH), 7.37 (s, 1H, 3-H), 6.58 (d, *J* = 1.6 Hz, 2H, 6-H), 6.49 (d, *J* = 1.6 Hz, 1H, 8-H), 4.67 (q, *J* = 7.1 Hz, 2H, NCH_2CH_3), 1.57 (s, 6H, $OC(CH_3)_2$), 1.58-1.47 (m, 2H, NCH_2CH_3), 1.44 (t, *J* = 7.1 Hz, 3H, 2′-H), 1.23 (s, 6H, $C(CH_3)_2$), 1.17 (bs, 6H, 3′-H, 4′-H and 5′-H), 1.07 (bs, 2H, 6′-H), 0.84-0.78 (m, 3H, 7′-H); ^{13}C NMR ($CDCl_3$): δ = 154.6 (9-C), 153.1 (5a-C), 151.67 (7-C), 133.1 (3-C), 132.2 (9b-C), 123.4 (3a-C), 108.8 (8-C), 108.0 (6-C), 103.2 (9a-C), 76.7 ($OC(CH_3)_2$), 48.4 (NCH_2CH_3), 44.8 (2′-C), 38.1 ($C(CH_3)_2$), 32.1, 30.4 and 25.01 (3′-C, 4′-C and 5-C), 29.0 ($C(CH_3)_2$), 27.7 ($OC(CH_3)_2$), 23.0 (6′-C), 16.3 (2′-C), 14.4 (7′-C); HPLC/MS: [A, 80% - 100%], Rt = 3.08 min, (99%); MS (ES^+, m/z) 371 (100%) $[M+H]^+$; Anal. calcd. for $C_{23}H_{34}N_2O_2$: C 74.55, H 9.25, found: C 74.63, H 9.19. **13b** was obtained as a white solid (23 mg, 61%); m.p.: 160-164 °C; ^{1}H NMR ($CDCl_3$): δ = 8.32 (s, 1H, OH), 7.13 (s, 1H, 3-H), 6.57 (d, *J* = 1.5 Hz, 8-H), 6.48 (s, 1H, *J* = 1.5 Hz, 6-H), 4.16 (q, 2H, *J* = 7.2 Hz, NCH_2CH_3), 1.60 (s, 6H, $OC(CH_3)_2$), 1.56 (bs, 2H, 2′-H), 1.50 (t, 2H, *J* = 7.2 Hz, NCH_2CH_3), 1.24 (s, 6H, $C(CH_3)_2$), 1.17 (bs, 6H, 3′-H, 4′-H and 5′-H), 1.01-0.96 (m, 2H, 6′-H), 0.86-79 (m, 3H, 7′-H); ^{13}C NMR ($CDCl_3$): δ = 153.6 (9-C), 153.2 (5a-C), 152.9 (7-C), 142.7 (9b-C), 122.8 (3-C), 120.3 (3a-C), 106.9 (6-C), 106.7 (8-C), 101.7 (9a-C), 76.4 ($OC(CH_3)_2$), 47.4 (NCH_2CH_3), 44.9 82(2′-C), 32.2, 30.4 and 30.1 (3′-C, 4′-C and 5′-C),

NIH-PA Author Manuscript

NIH-PA Author Manuscript

NIH-PA Author Manuscript

29.3 ($C(CH_3)_2$), 25.0 ($OC(CH_3)_2$), 23.1 (6′-C), 15.9 (NCH_2CH_3), 14.5 (7′-C); HPLC/MS: [A, 80% - 100%], Rt = 5.6 min, (98%); MS (ES^+, m/z) 371 (100%) $[M+H]^+$; Anal. calcd. for $C_{23}H_{34}N_2O_2$: C 74.55, H 9.25, found: C 74.23, H 9.41.

1-(3,4-Dichlorophenyl)-7-(1,1-dimethylheptyl)-1,4-dihydro-4,4-dimethylchromeno[4,3-*c*]pyrazol-9-ol (14a)

Prepared from **6** (17.0 mg, 0.05 mmol) and 3,4-dichlorophenylhydrazine hydrochloride (10.0 mg, 0.05 mmol) following the procedure described for **7**. Column chromatography on silica gel (Hex/EtOAc, 2/1) afforded **14a** as an orange solid (9 mg, 40%); mp: 124-126 °C; ^{1}H NMR ($CDCl_3$): δ = 7.65 (d, *J* = 2.3 Hz, 1H, 2-H_{phenyl}), 7.50 (s, 1H, 3-H), 7.43 (d, *J* = 8.5 Hz, 1H, 5-H_{phenyl}), 7.25 (dd, *J* = 2.3 Hz, *J* = 8.5 Hz, 1H, 6-H_{phenyl}), 6.66 (d, *J* = 1.6 Hz, 1H, 6-H), 6.24 (d, *J* = 1.6 Hz, 1H, 8-H), 1.68 (s, 6H, $OC(CH_3)_2$), 1.60-1.54 (m, 2H, 2′-H), 1.22 (s, 6H, $C(CH_3)_2$), 1.20-1.09 (m, 6H, 3′-H, 4′-H and 5′-H), 1.08-1.02 (m, 2H, 6′-H), 0.84 (t, *J* = 6.5 Hz, 3H, 7′-H); ^{13}C NMR ($CDCl_3$): δ = 154.6 (9-C), 154.0 (5a-C), 150.0 (7-C), 142.3 (1-C_{phenyl}), 135.3 (3-C), 133.2 (3-C_{phenyl}), 132.2 (9b-C), 130.4 (4-C_{phenyl}), 126.5 (5-C_{phenyl}), 125.4 (2-C_{phenyl}), 123.9 (6-C_{phenyl}), 109.6 (6-C), 108.0 (8-C), 102.4 (9a-C), 76.2 ($OC(CH_3)_2$), 44.7 (2′-C), 38.3 ($C(CH_3)_2$), 32.1, 30.3 and 25.0 (3′-C, 4′-C and 5′-C), 28.9 ($C(CH_3)_2$), 27.7 ($OC(CH_3)_2$, 23.0 (6′-C), 14.5 (7′-C); HPLC/MS: [A, 80% - 100%], Rt = 5.6 min, (98%); MS (ES^+, m/z) 487 (100%) $[M+H]^+$.

1-(2,4-Dichlorophenyl)-7-(1,1-dimethylheptyl)-1,4-dihydro-4,4-dimethylchromeno[4,3-*c*]pyrazol-9-ol (15a)

Prepared from **6** (0.05 mg, 0.16 mmol) and 2,4-dichlorophenylhydrazine hydrochloride (0.13 g, 0.63 mmol) following the procedure described for **7**. Column chromatography on silica gel (Hex/EtOAc, 2/1) afforded **15a** as an orange oil (0.06 g, 75%); ^{1}H NMR ($CDCl_3$): δ = 7.43 (s, 1H, 3-H), 7.39 (d, *J* = 2.2 Hz, 1H, 3-H_{phenyl}), 7.27 (dd, *J* = 2.2 Hz, *J* = 8.7 Hz, 1H, 5-H_{phenyl}), 7.21 (d, *J* = 8.7 Hz, 1H, 6-H_{phenyl}), 6.56 (d, *J* = 1.6 Hz, 1H, 6-H), 6.12 (d, *J* = 1.6 Hz, 1H, 8-H), 1.64 (s, 6H, $OC(CH_3)_2$), 1.46-1.41 (m, 2H, 2′-H), 1.16-1.08 (m, 12H, 3′-H, 4′-H, 5′-H and $C(CH_3)_2$), 1.12-0.98 (m, 2H, 6′-H), 0.82 (t, *J* = 6.9 Hz, 3H, 7′-H); ^{13}C NMR ($CDCl_3$): δ = 154.3 (9-C), 153.6 (5a-C), 151.3 (7-C), 140.3 (1-C_{phenyl}), 135.3 (2-C_{phenyl}), 135.0 (4-C_{phenyl}) , 134.4 (3-C), 133.0 (9b-C), 129.8 (3-C_{phenyl}), 129.6 (5-C_{phenyl}), 127.3 (6-C_{phenyl}), 123.4 (3a-C), 108.8 (6-C), 107.6 (8-C), 102.6 (9a-C), 77.6 ($OC(CH_3)_2$), 44.7 (2′-C), 39.1 ($C(CH_3)_2$), 32.1 , 30.3 and 24.9 (3′-C, 4′-C and 5′-C), 28.9 ($C(CH_3)_2$), 28.0 ($OC(CH_3)_2$), 23.0 (6′-C), 14.5 (7′-C); HPLC/MS: [A, 20% - 80%], Rt = 19.0 min, (99%); MS (ES^+, m/z) 487 (100%) $[M+H]^+$.

Biological studies

Binding Evaluation

Membranes from transfected cells with human CB_1 or CB_2 expressed cannabinoid receptors (RBHCB1M400UA and RBXCB2M400UA) were supplied by Perkin-Elmer Life and Analytical Sciences (Boston, MA). The CB_1 receptor membrane proteins concentration was 2.33 pmol/mg or 3.60 pmol/mg depending on the batch and the protein concentration was 8.0 mg/ml. The CB_2 receptor membrane protein concentration was 5.20 pmol/mg or 6.20 pmol/mg and the protein concentration was 4.0 mg/ml or 3.6 mg/ml depending on the batch.

NIH-PA Author Manuscript

NIH-PA Author Manuscript

NIH-PA Author Manuscript

The commercial membranes were diluted (approximatively1:20) with the binding buffer (50 mM TrisCl, 5 mM $MgCl_2.H_2O$, 2.5 mM EDTA, 0.5 mg/mL BSA and pH = 7.4 for CB_1 binding; 50 mM TrisCl, 5 mM $MgCl_2.H_2O$, 2.5 mM EGTA, 1 mg/mL BSA and pH = 7.5 for CB_2 binding). The final membrane protein concentration was 0.4 mg/mL of incubation volume and 0.2 mg/mL of incubation volume for the CB_1 and the CB_2 receptor assays, respectively. The radioligand used was [^{3}H]-CP55940 (PerkinElmer) at a concentration of membrane K_D × 0.8 nm, and the final volume was 200 μL for CB_1 binding and was 600 μL for CB_2 binding. 96-Well plates and the tubes necessary for the experiment were previously siliconized with Sigmacote (Sigma).

Membranes were resuspended in the corresponding buffer and were incubated with the radioligand and each compound (10^{-4}-10^{-11} M) for 90 min at 30 °C. Non-specific binding was determined with 10 μM WIN55212-2 and 100 % binding of the radioligand to the membrane was determined by its incubation with membrane without any compound. Filtration was performed by a Harvester® filtermate (Perkin-Elmer) with Filtermat A GF/C filters pretreated with polyethylenimine 0.05%. After filtering, the filter was washed nine times with binding buffer, dried and a melt-on scintillation sheet (Meltilex™ A, Perkin Elmer) was melted onto it. Then, radioactivity was quantified by a liquid scintillation spectrophotometer (Wallac MicroBeta Trilux, Perkin-Elmer). Competition binding data were analyzed by using GraphPad Prism program and K_i values are expressed as mean ± SD of at least three experiments performed in triplicate for each point.

Isolated tissues assays

Compounds **11**, **13a** and **13b** were evaluated on the mouse vas deferens preparation. This is a nerve-smooth muscle preparation that serves as a highly sensitive and quantitative functional in vitro bioassay for cannabinoid receptor agonists. These ligands induce concentration-related decrease in the amplitude of electrically evoked contractions of the vas deferens by acting on naturally expressed prejunctional neuronal cannabinoid receptors to inhibit release of the contractile neurotransmitters, noradrenaline and ATP, that is provoked by the electrical stimulation.[47-48] For this study, male ICR mice weighing 25–30 g were used. Mouse vas deferens were isolated as described by Hughes.[49] Tissues were suspended in a 10 mL organ bath containing 5 mL of Krebs solution (NaCl 118; KCl 4.75; $CaCl_2$ 2.54; KH_2PO_4 1.19; $MgSO_4$ 1.2; $NaHCO_3$ 25; glucose 11 mM) that was continuously gassed with 95% O_2 and 5% CO_2. Tissues were kept under 0.5 g of resting tension at 37 °C and were electrically stimulated through two platinum ring electrodes. They were subjected to alternate periods of stimulation (trains of five rectangular pulses of 70 V, 15 Hz and 2 ms duration each were applied every minute) and rest (10 min). The isometric force was monitored by computer using a MacLab data recording and analysis system.

The effect of the synthetic cannabinoid agonists arachidonyl-2-chloroethylamide (ACEA), WIN 55,212-2 and that of the new compounds **11**, **13a** and **13b** (10^{-7}–1.8×10^{-5} M) was tested by constructing concentration–response curves for them in a step by step manner. Curves were carried out by the following protocol: ACEA, WIN 55,212-2 or the new compounds were added at a dose to the organ bath 50 min after the beginning of electrical stimulation and their effect on the electrically induced contractions was evaluated 10 min

NIH-PA Author Manuscript

NIH-PA Author Manuscript

NIH-PA Author Manuscript

after their addition. Then, the electrical stimulation was stopped, Krebs solution was replaced and the following dose of the compounds was added. This protocol was repeated for every dose.

To test the involvement of the CB_1 and CB_2 receptors in the effect of **13a**, it was tested in tissues incubated with the cannabinoid antagonists AM251 or AM630 (10^{-6} M) respectively. Concentration–response curves for the new compound were constructed in a step by step manner as follows: AM251 or AM630 was added to the organ bath 50 min after the beginning of electrical stimulation and 10 minutes later, a dose of **13a** was added and its effect on the electrically induced contractions was tested 10 min later. Then, the electrical stimulation was stopped, Krebs solution was replaced and the cannabinoid receptor antagonist was added again to test the effect of the following concentration of the new compound. This protocol was repeated for every dose of **13a**. Results have been expressed as % of inhibition, taking the mean amplitude of the last five contractions before the first addition of the agonist as 100%. Each tissue was employed to construct only one concentration–response curve.

In vivo behavioural studies

Behavioural testing of cannabinoids is performed in order to assess psychoactive drug potential, central side effects, as well as medicinal potential. The compound **13a** was evaluated in tests of CNS activity, using the mouse cannabinoid tetrad. The potential antinociceptive effect was also evaluated in an orofacial pain model, induced by hypertonic saline (HS).

Animals

ICR male mice (25-30 g) and Wistar male rats (250-300 g), purchased at Harlan, S.A., were used in cannabinoid tetrad and orofacial pain model, respectively. Animals were supplied with food and water “ad libitum” and were housed in a temperature-controlled room at 23 ± 1°C under a standard 12/12-h light/dark cycle (08:00-20:00 h); they were housed in the test room for at least two days before experimentation. Throughout the experimental procedure, the international ethics standards for pain-inducing experiments in laboratory animals[50] and the European Communities Council Directive of 24 November 1986 (86/609 EEC, Nov 24, 1986) were followed. All animal procedures were reviewed and approved by the Animal Care and Use Committee of Rey Juan Carlos University.

Drugs

WIN 55,212-2 and the compound **13a** were dissolved in ethanol 1 mg:1 ml and subsequently in ethanol and Tween 80 (1:2), after which the ethanol was evaporated and saline solution added to reach the final concentration.[47] All solutions were made fresh before each experiment.

Cannabinoid tetrad

The classical cannabinoid tetrad was performed to study SNC side effects; this test evaluates antinociception, hypothermia, catalepsy and locomotor activity in the same animal 20 minutes after cannabinoid administration.[51] Separated groups of mice ($n \geq 10$) were

NIH-PA Author Manuscript

NIH-PA Author Manuscript

NIH-PA Author Manuscript

intraperitoneally treated with vehicle, WIN55,212-2 (2.5 and 5 mg/kg) and compound **13a** (5 and 10 mg/kg). Tests were consecutively conducted with 5 minutes of interval between them.

Antinociception

The hot-plate test was carried out using a hot-plate at 55 °C as nociceptive stimulus. The latency time of licking of the front paw was taken as an index of nociception. The latency was measured before treatment (control latency) and after every treatment (latency after treatment). The cut-off time was 30 s and analgesia was quantified with the formula of the Maximum Possible Effect (M.P.E.), expressed as a percentage: % M.P.E. = (Latency after treatment - Control Latency) / (Cut-off time - Control latency) × 100.

Hypothermia

Core temperatures in mice were measured using a P6 thermometer and a lubricated rectal probe (CIBERTEC, Spain) inserted into the rectum at a constant depth of 1 cm. Data were recorded before and 30 min after treatment.

Catalepsy

Catalepsy was measured using a modified “ring test”, originally described by Pertwee.[51] Mice were placed on a rubber coated metal ring (6 cm diameter) fixed horizontally at a height of 30 cm. The amount of time in which the mouse is immobile after placement on the ring is recorded for 5 min, and it is considered as an index of catalepsy.

Locomotor activity

Motor coordination was assessed using the rota-rod test (Cibertec, Madrid, Spain), in which mice were required to walk against the motion of an rotating drum with a constant speed of rotation of 10 revolutions/min over 5 min. The time (in s) taken to fall down was recorded as the latency. Animals were trained to the rota-rod test before the pharmacological assay. On the day of the drug test rota-rod latencies were measured immediately before the drug or vehicle was given and 30 min after the drug injection. In all experiments we used a 300-s cut-off time and to this time is given a value of 100 % of locomotor activity.

Orofacial pain model

The injection of 100 μl of HS (5% NaCl) in the masseter of lightly anesthetised rats produces ipsilateral hindpaw shaking behaviour that is accepted as an index of muscle nociception.[46, 52-53] Separated groups of rats ($n \geq 10$) were intraperitoneally (i.p.) treated with the vehicle, and compound **13a** (1-3 mg/kg) and 30 min after HS was injected in the masseter. Shaking behaviour was quantified by counting the total number of shakes in a 2-min period after the intramuscular injection of HS. To count the number of shakes, the experiments were recorded on video and then played back in slow motion.

NIH-PA Author Manuscript

NIH-PA Author Manuscript

NIH-PA Author Manuscript

Molecular modeling

Amino acid numbering

The numbering scheme for Class A GPCRs suggested by Ballesteros and Weinstein[54] was employed here. In this system, the most highly conserved residue in each TMH is assigned a locant of 0.50. This number is preceded by the TMH number and followed in parenthesis by the sequence number. All other residues in a TMH are numbered relative to this residue.

Conformational analysis of 11 and 13a/13b

Global minimum energy conformations of **11** and **13a/13b** were determined with Spartan ′04 as follows: the structure of each molecule was built from the fragment library available in the program. Then, ab initio energy minimizations of each structure (HF 6-31G*) were performed. A conformational search was next performed using Spartan ′04 (Monte Carlo method) followed by a minimization of the energy of each conformer at the semiempirical PM3 level. For this search, selected bonds were allowed to rotate: C-O bond in the phenolic ring, the first two C-C bonds of the dimethylheptyl chain, and the N-C bond in the ethyl substituent of the pyrazole, in the case of **13a** and **13b**. Representative conformers according to their geometry were selected for ab initio energy minimization (HF 6-31G*), the global minimum energy conformer of each was used in docking studies.

Docking with CB_1R*

Binding site anchoring interactions within the receptor for each ligand were based on earlier published docking studies for HU210.[38] Lys3.28(192) was used as the primary interaction site for the phenolic hydroxyl of each chromenopyrazole. Mutation of this residue in CB1 results in the loss of binding of classical, non-classical and endocannabinoids, suggesting that interaction with K3.28 is crucial for binding of this class of ligand.[41] The energy of the ligand/CB_1R* TMH bundle complex was minimized using the OPLS2005 force field in Macromodel 9.1 (Schrödinger Inc., Portland, OR). An 8.0-Å extended nonbonded cutoff (updated every 10 steps), a 20.0- Å electrostatic cutoff, and a 4.0-Å hydrogen bond cutoff were used in each stage of the calculation. 7000 steps of conjugate gradient minimization in 500-step (6 times) increments followed by 1000-step (4 times) increments were employed in a distance-dependent dielectric. A 100 kJ/mol restraint was placed on all ϕ and ψ angles in TMH1-7 and Hx 8 and a 50 kJ/mol restraint was placed on Lys3.28(192)-phenolic OH hydrogen bond.

Energy expense assessments for docked ligands

To calculate the energy difference between the global minimum energy conformer of each compound and its final conformation after energy minimization of the ligand/receptor complex, rotatable bonds in the global minimum energy conformation were driven to their corresponding value in the final docked conformation and the single point energy of the resultant structure was calculated at the HF 6-31G* level using Jaguar (implemented in Maestro 8.5, Schrödinger).

NIH-PA Author Manuscript

NIH-PA Author Manuscript

NIH-PA Author Manuscript

Docking in CB_2R*

Global minimum conformations of each ligand were superimposed on HU210 in its complex with the CB_2R* model (unpublished results). Benzopyran atoms of **14** and **16a/b** were selected for superimposition with benzopyran ones of HU210. The conformation of the 1,1-dimethylheptyl side chain in the HU210/ CB_2R* complex was used to overlay the 1,1-dimethylheptyl side chain position of **11** and **13a/b**. After the superimposition, HU210 was removed. The pyrazole ring of the chromenopyrazoles ligands all had steric clashes with the Asp275 /Lys3.28(109) salt bridge. Changes in side chain dihedrals of these two residues were attempted to relieve the steric overlaps, however it was impossible to relieve this clash without disrupting this ionic lock.

Assessment of Pair-wise Interaction Energies

After defining the atoms of each ligand as one group (Group 1) and the atoms corresponding to a residue that lines the binding site in the final ligand/CB_1 R complex as another group (Group 2), Macromodel (version 8.6, Schrödinger, LLC, New York, NY) was used to output the pair-wise interaction energy (coulombic and Van der Waals) for a given pair of atoms. The pairs corresponding to Group 1 (ligand) and Group 2 (residue of interest) were then summed to yield the interaction energy between the ligand and that residue.

Supplementary Material

Refer to Web version on PubMed Central for supplementary material.

Acknowledgments

We gratefully acknowledge the research support from Spanish Grant SAF 2009-12422-C02-02, CANNAB-CM (S-SAL-0261-2006) and RTA (RETICS RD06/001/0014) to P.G. and N.J. L.H.-F. and P.M. are respectively recipient of a Postdoctoral Contract (ref JAEDoc-07-00204) and a JAE-Pre Fellowship (ref JAEPre-2010-01119) from C.S.I.C.

References

[1]. Gertsch J, Pertwee RG, Di Marzo V. Br. J .Pharmacol. 2010; 160:523–529. [PubMed: 20590562]
[2]. Gaoni Y, Mechoulam R. J. Am. Chem. Soc. 1971; 93:217–224. [PubMed: 5538858]
[3]. Pertwee RG. Br. J. Pharmacol. 2006; 147(Suppl 1):S163–171. [PubMed: 16402100]
[4]. Pertwee RG. Pharmacol. Ther. 1997; 74:129–180. [PubMed: 9336020]
[5]. Mackie K. J. Neuroendocrinol. 2008; 20(Suppl 1):10–14. [PubMed: 18426493]
[6]. Hanus LO, Mechoulam R. Curr. Med. Chem. 2010; 17:1341–1359. [PubMed: 20166928]
[7]. Marriott KS, Huffman JW. Curr. Top. Med. Chem. 2008; 8:187–204. [PubMed: 18289088]
[8]. Jagerovic N, Fernandez-Fernandez C, Goya P. Curr. Top. Med. Chem. 2008; 8:205–30. [PubMed: 18289089]
[9]. Woelkart K, Salo-Ahen OM, Bauer R. Curr. Top. Med. Chem. 2008; 8:173–186. [PubMed: 18289087]
[10]. Pertwee RG. Br. J. Pharmacol. 2009; 156:397–411. [PubMed: 19226257]
[11]. Pavlopoulos S, Thakur GA, Nikas SP, Makriyannis A. Curr. Pharm. Des. 2006; 12:1751–1769. [PubMed: 16712486]
[12]. Di Marzo V, Bifulco M, De Petrocellis L. Nat. Rev. Drug Discov. 2004; 3:771–784. [PubMed: 15340387]

NIH-PA Author Manuscript

NIH-PA Author Manuscript

NIH-PA Author Manuscript

[13]. Appendino G, Chianese G, Taglialatela-Scafati O. Curr. Med. Chem. 2011; 18:1085–1099. [PubMed: 21254969]

[14]. Thakur GA, Nikas SP, Makriyannis A. Mini Rev. Med. Chem. 2005; 5:631–640. [PubMed: 16026309]

[15]. Thakur GA, Nikas SP, Li C, Makriyannis A. Handb Exp. Pharmacol. 2005:209–246. [PubMed: 16596776]

[16]. Thakur GA, Duclos RI Jr. Makriyannis A. Life Sci. 2005; 78:454–466. [PubMed: 16242157]

[17]. Palmer SL, Thakur GA, Makriyannis A. Chem. Phys. Lipids. 2002; 121:3–19. [PubMed: 12505686]

[18]. Huffman JW, Miller JR, Liddle J, Yu S, Thomas BF, Wiley JL, Martin BR. Bioorg. Med. Chem. 2003; 11:1397–1410. [PubMed: 12628666]

[19]. Huffman JW, Yu S, Showalter V, Abood ME, Wiley JL, Compton DR, Martin BR, Bramblett RD, Reggio PH. J. Med. Chem. 1996; 39:3875–3877. [PubMed: 8831752]

[20]. Rhee MH, Vogel Z, Barg J, Bayewitch M, Levy R, Hanus L, Breuer A, Mechoulam R. J. Med. Chem. 1997; 40:3228–3233. [PubMed: 9379442]

[21]. Mahadevan A, Siegel C, Martin BR, Abood ME, Beletskaya I, Razdan RK. J. Med. Chem. 2000; 43:3778–3785. [PubMed: 11020293]

[22]. Khanolkar AD, Lu D, Ibrahim M, Duclos RI Jr. Thakur GA, Malan TP Jr. Porreca F, Veerappan V, Tian X, George C, Parrish DA, Papahatjis DP, Makriyannis A. J. Med. Chem. 2007; 50:6493–6500. [PubMed: 18038967]

[23]. Sofia RD, Vassar HB, Knobloch LC. Psychopharmacologia. 1975; 40:285–95. [PubMed: 1170585]

[24]. Welburn PJ, Starmer GA, Chesher GB, Jackson DM. Psychopharmacologia. 1976; 46:83–85. [PubMed: 1257370]

[25]. Booker L, Naidu PS, Razdan RK, Mahadevan A, Lichtman AH. Drug Alcohol Depend. 2009; 105:42–47. [PubMed: 19679411]

[26]. Sanders J, Jackson DM, Starmer GA. Psychopharmacology (Berl). 1979; 61:281–5. [PubMed: 156380]

[27]. Petitet F, Jeantaud B, Bertrand P, Imperato A. Eur. J. Pharmacol. 1999; 374:417–421. [PubMed: 10422786]

[28]. Steger RW, Murphy LL, Bartke A, Smith MS. Pharmacol. Biochem. Behav. 1990; 37:299–302. [PubMed: 1964220]

[29]. Press JB, Birnberg GH. J. Heterocycl. Chem. 1985; 22:561–564.

[30]. Dominianni SJ, Ryan CW, DeArmitt CW. J. Org. Chem. 1977; 42:344–346. [PubMed: 830862]

[31]. Lim J, Kim I-H, Kim HH, Ahn K-S, Han H. Tetrahedron Lett. 2001; 42:4001–4003.

[32]. Press JB, McNally JJ, Sanfilippo PJ, Addo MF, Loughney D, Giardino E, Katz LB, Falotico R, Haertlein BJ. Bioorg. Med. Chem. 1993; 1:423–435. [PubMed: 8087564]

[33]. Loev B, Bender PE, Dowalo F, Macko E, Fowler PJ. J. Med. Chem. 1973; 16:1200–1206. [PubMed: 4795866]

[34]. Jagerovic N, Hernandez-Folgado L, Alkorta I, Goya P, Navarro M, Serrano A, de Fonseca FR, Dannert MT, Alsasua A, Suardiaz M, Pascual D, Martin MI. J. Med. Chem. 2004; 47:2939–2942. [PubMed: 15139773]

[35]. Compton DR, Rice KC, Decosta BR, Razdan RK, Melvin LS, Johnson MR, Martin BR. J. Pharmacol. Exp. Ther. 1993; 265:218–226. [PubMed: 8474008]

[36]. Reggio PH. Handb Exp. Pharmacol. 2005:247–281. [PubMed: 16596777]

[37]. Hurst DP, Grossfield A, Lynch DL, Feller S, Romo TD, Gawrisch K, Pitman MC, Reggio PH. J. Biol. Chem. 2010; 285:17954–17964. [PubMed: 20220143]

[38]. Kapur A, Hurst DP, Fleischer D, Whitnell R, Thakur GA, Makriyannis A, Reggio PH, Abood ME. Mol. Pharmacol. 2007; 71:1512–1524. [PubMed: 17384224]

[39]. Nebane NM, Hurst DP, Carrasquer CA, Qiao Z, Reggio PH, Song ZH. Biochemistry. 2008; 47:13811–13821. [PubMed: 19053233]

NIH-PA Author Manuscript

NIH-PA Author Manuscript

NIH-PA Author Manuscript

[40]. Pei Y, Mercier RW, Anday JK, Thakur GA, Zvonok AM, Hurst D, Reggio PH, Janero DR, Makriyannis A. Chem. Biol. 2008; 15:1207–1219. [PubMed: 19022181]

[41]. Song ZH, Bonner TI. Mol. Pharmacol. 1996; 49:891–896. [PubMed: 8622639]

[42]. Zhang R, Hurst DP, Barnett-Norris J, Reggio PH, Song ZH. Mol. Pharmacol. 2005; 68:69–83. [PubMed: 15840841]

[43]. Cheng Y, Hitchcock SA. Expert Opin. Investig. Drugs. 2007; 16:951–65.

[44]. Tao Q, McAllister SD, Andreassi J, Nowell KW, Cabral GA, Hurst DP, Bachtel K, Ekman MC, Reggio PH, Abood ME. Mol. Pharmacol. 1999; 55:605–613. [PubMed: 10051546]

[45]. Sánchez EBA, Martín MI. Pharmacol. Biochem. Behav. 2010; 96:488–495. [PubMed: 20637793]

[46]. Han SR, Lee MK, Lim KH, Yang GY, Jeon HJ, Ju JS, Yoon YW, Kim SK, Ahn DK. Eur. J. Pain. 2008; 12:361–370. [PubMed: 17768078]

[47]. Pertwee RG, Stevenson LA, Elrick DB, Mechoulam R, Corbett AD. Br. J. Pharmacol. 1992; 105:980–984. [PubMed: 1324060]

[48]. Thomas A, Pertwee RG. Methods Mol. Med. 2006; 123:191–207. [PubMed: 16506409]

[49]. Hughes J, Kosterlitz HW, Leslie FM. Br. J. Pharmacol. 1975; 53:371–381. [PubMed: 236796]

[50]. Zimmermann M. Pain. 1983; 16:109–110. [PubMed: 6877845]

[51]. Pertwee RG. Br. J. Pharmacol. 1972; 46:753–763. [PubMed: 4655271]

[52]. Sanchez EM, Bagues A, Martin MI. Pharmacol. Biochem. Behav. 2010; 96:488–495. [PubMed: 20637793]

[53]. Ro JY, Capra N, Masri R. Pain. 2003; 104:179–185. [PubMed: 12855327]

[54]. Ballesteros, JA.; Weinstein, H. Methods in Neurosciences. Conn, PM.; Sealfon, SM., editors. Academic Press; San Diego: 1995. p. 366-428.

NIH-PA Author Manuscript

NIH-PA Author Manuscript

NIH-PA Author Manuscript

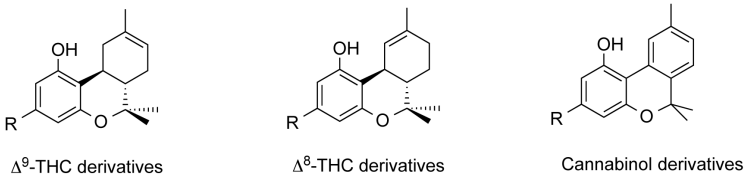

Figure 1.
Chemical structures of Δ^9–THC, Δ^8-THC and cannabinol derivatives.

NIH-PA Author Manuscript

NIH-PA Author Manuscript

NIH-PA Author Manuscript

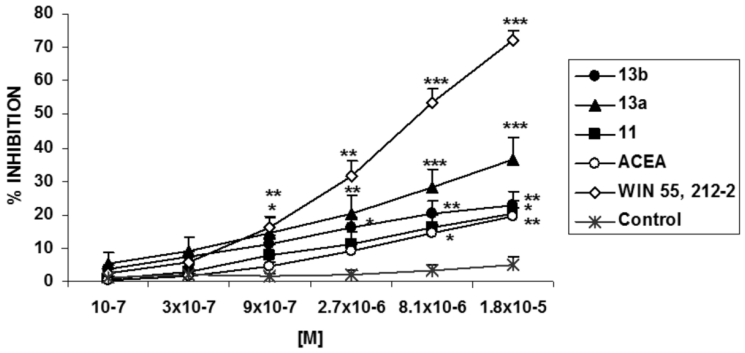

Figure 2.

Effect of WIN55, 212-2 (WIN), arachidonyl-2-chloroethylamide (ACEA) and compounds **11**, **13a** and **13b** in mouse vas deferens. Lines show the means % ± S.E.M. (n = 6-8) of modification of the electrically induced contraction of the mouse vas deferens by addition of increasing concentrations of vehicle (Control), WIN, ACEA or the new compounds **11**, **13a** and **13b**. The * represent the significant difference versus Control: *p<0.05, **p < 0.01, ***p< 0.001 (Two-ways ANOVA followed by Bonferroni′s post-hoc test).

NIH-PA Author Manuscript
NIH-PA Author Manuscript
NIH-PA Author Manuscript

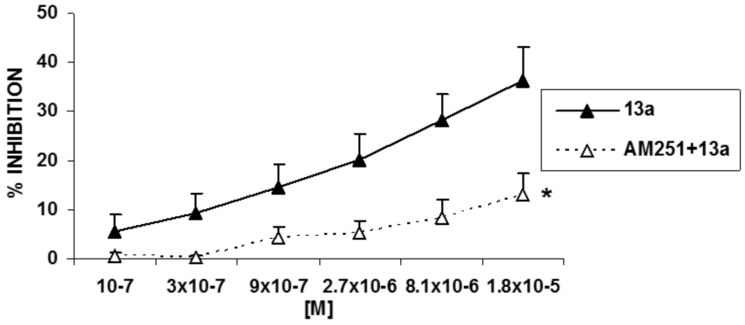

Figure 3.

Lines show the mean % ± S.E.M. (n = 6) inhibition of the electrically induced contraction of the mouse vas deferens induced by addition of increasing concentrations of compound **13a** in control tissues or in tissues incubated with AM251. The * represent the significant difference versus control tissues: *p<0.05 (Two-ways ANOVA followed by Bonferroni′s post-hoc test).

NIH-PA Author Manuscript

NIH-PA Author Manuscript

NIH-PA Author Manuscript

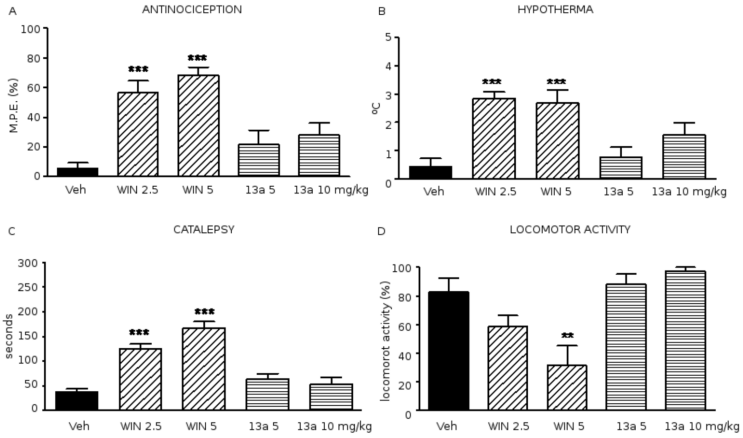

Figure 4.

Effect of WIN 55,212-2 (WIN) (2.5 and 5 mg/kg) and compound **13a** (5 and 10 mg/kg) in the mouse cannabinoid tetrad. Mice were tested for analgesia on a hot-plate (A), rectal temperature (B), catalepsy on a ring (C) and locomotor activity on the rota-rod test (D). ** $p<0.01$, *** $p<0.001$ vs vehicle (Veh). One-way ANOVA, n ≥10

NIH-PA Author Manuscript

NIH-PA Author Manuscript

NIH-PA Author Manuscript

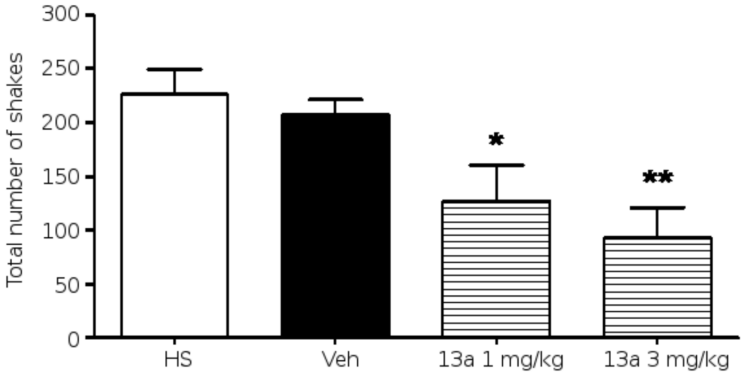

Figure 5.

Antinociceptive effect of compound **13a** (1 and 3 mg/kg), i.p.administered, 30 min before HS injection. Bars show the total number of shakes (mean ± SEM). * $p<0.05$, ** $p<0.01$ vs vehicle (Veh) (One-way ANOVA, n ≥6)

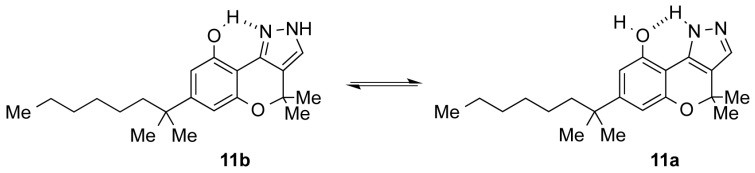

Figure 6.
Molecular structure of the two tautomers **11b** and **11a**.

NIH-PA Author Manuscript
NIH-PA Author Manuscript
NIH-PA Author Manuscript

NIH-PA Author Manuscript

NIH-PA Author Manuscript

NIH-PA Author Manuscript

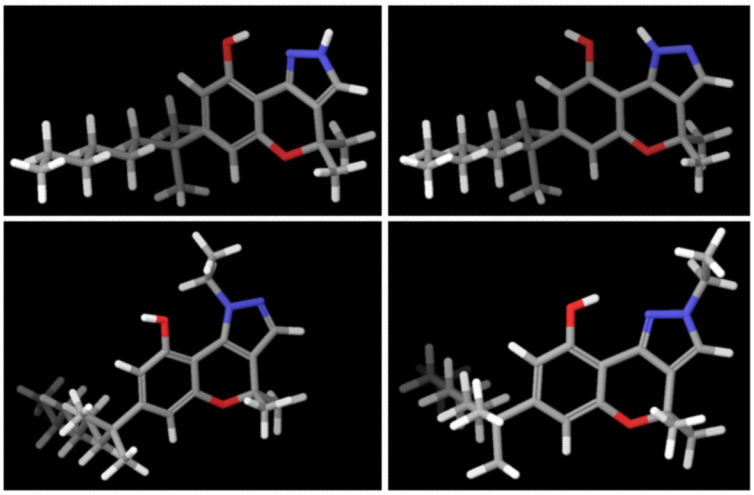

Figure 7.
Minimum energy conformers of tautomers **11a**, **11b**, **13a**, and **13b**.

NIH-PA Author Manuscript
NIH-PA Author Manuscript
NIH-PA Author Manuscript

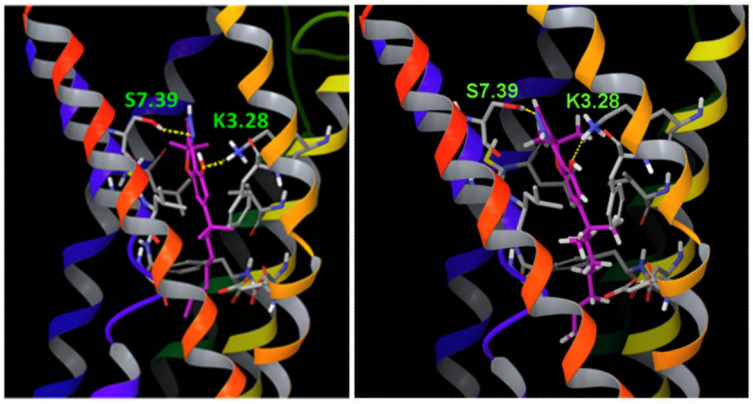

Figure 8.

Binding site of **11b** (left, in pink) and **11a** (right, in pink) in the CB_1R^* model. The amino acid residues interacting with the ligand are shown in grey. Yellow dashed lines indicate hydrogen bonding interactions.

NIH-PA Author Manuscript

NIH-PA Author Manuscript

NIH-PA Author Manuscript

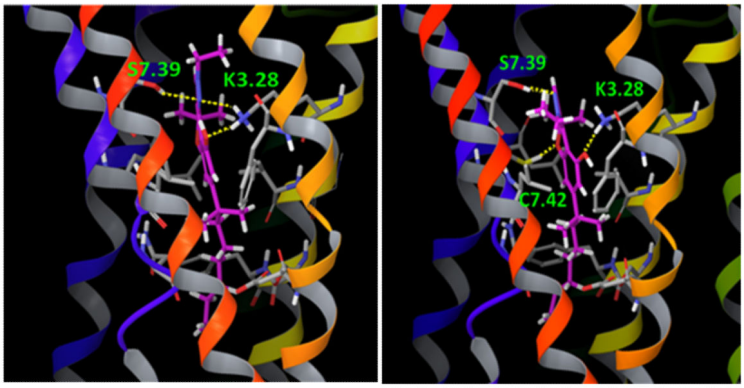

Figure 9.

Binding site of **13a** (left, in pink) and **13b** (right, in pink) in the CB_1R* model. The amino acid residues interacting with the ligand are shown in grey. Yellow dashed lines indicate hydrogen bonding interactions.

NIH-PA Author Manuscript

NIH-PA Author Manuscript

NIH-PA Author Manuscript

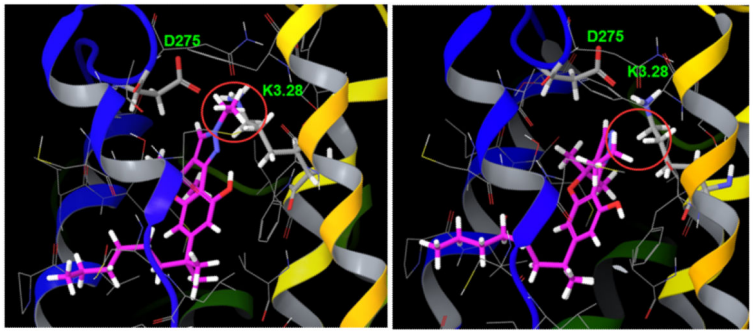

Figure 10.

Binding site of **13b** (left, in pink) and **13a** (right, in pink) in the CB_2R* model. The D275-K3.28(109) ionic lock is shown in grey. Red circle indicate steric clash.

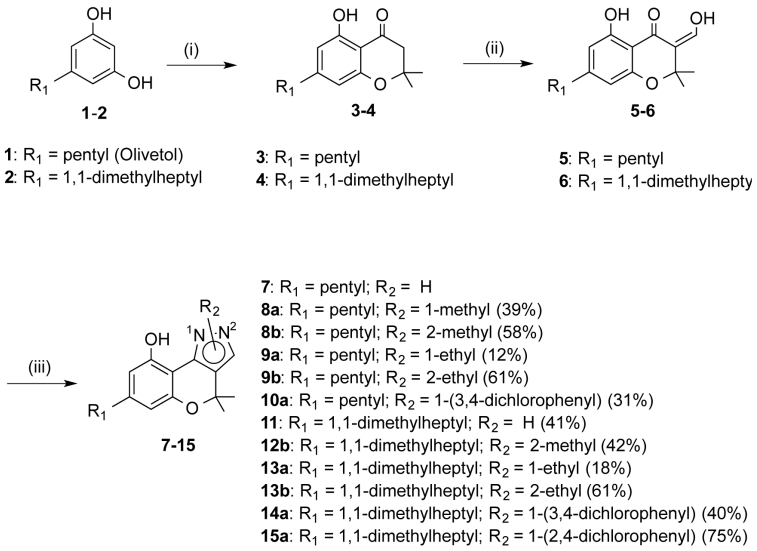

Scheme 1.

Reagents and conditions: (i) 3,3-dimethylacrylic acid, CH_3SO_3H, P_2O_5, 70 °C, M.W., 10 min; (ii) NaH, THF, M.W., 46°C, 20 min then ethyl formate, THF, M.W., 46°C, 20 min; (iii) $H_2N\text{-}NHR_2$, EtOH, 16 h at room temperature or 10 min under M.W.

NIH-PA Author Manuscript NIH-PA Author Manuscript NIH-PA Author Manuscript

NIH-PA Author Manuscript
NIH-PA Author Manuscript
NIH-PA Author Manuscript

Table 1

Binding Affinity K_i Values of Chromenopyrazole Derivatives **7-15** at *h*CB_1 and *h*CB_2 Cannabinoid Receptors. *[a]*

compd	R^1	R^2	hCB_1 K_i (nM)	hCB_2 K_i (nM)	CB_1/CB_2 [c]
7	pentyl	H	4100±800	2010±500	0.5
8a	pentyl	1-methyl	4700±1200	3460±1000	0.7
8b	pentyl	2-methyl	22100±1410	>40000	-
9a	pentyl	1-ethyl	9610	>40000	-
9b	pentyl	2-ethyl	>40000	4450±1015	-
10a	pentyl	1-(3,4-dichlorophenyl)	607±151	>40000	-
11	1,1-dimethylheptyl	H	28.5±33.6	>40000	>1000
12b	1,1-dimethylheptyl	2-methyl	14.2±4.2	>40000	>1000
13a	1,1-dimethylheptyl	1-ethyl	4.5±0.8	>40000	>1000
13b	1,1-dimethylheptyl	2-ethyl	18.6±4.1	>40000	>1000
14a	1,1-dimethylheptyl	1-(3,4-dichlorophenyl)	514±355	270	0.5
15a	1,1-dimethylheptyl	1-(2,4-dichlorophenyl)	5.2±6.0	>40000	>1000
SR141716			7.3±0.9	ND[b]	
WIN55,212-2			45.6±8.6	3.7±0.2	

[a] K_i values obtained from competition curves using as [^{3}H]-CP55940 radioligand for hCB_1 and hCB_2 cannabinoid receptors. The values are expressed as mean ± SEM of at least three experiments.

b ND:not determined.

c Selectivity ratio CB_1 versus CB_2.